Vibration Analysis of Laminated Composite Thin-Walled Beams Using Finite Elements

X. X. Wu* and C. T. Sun†
Purdue University, West Lafayette, Indiana 47907

A two-noded, 10 degree of freedom per node, laminated composite thin-walled beam finite element was developed for vibration analysis. The thin-walled element presented here is suitable for either open-section or closed-section beams of any shape, stacking sequence, and boundary conditions. Natural frequencies of several thin-walled composite structures were calculated and compared with full-scale shell finite element results.

Introduction

THE theory of isotropic thin-walled beams has been well developed by a large number of researchers. Vlasov,[1] Timoshenko,[2] and Gjelsvik[3] obtained solutions to the problem of isotropic thin-walled beams by deriving differential equations with varying degrees of accuracy. Bauld and Tzeng[4] established a Vlasov-type theory for thin-walled beams with open cross sections made from midplane symmetric, fiber-reinforced laminates. Krahula,[5] Krajcinovic,[6] and Yoo[7] presented finite element formulations for thin-walled, open-section beams of isotropic material based on the solutions of the governing differential equations. Consequently, the displacement field and elements of the stiffness matrices have hyperbolic terms in their expressions, and mesh refinement is not necessary. Barsoum and Gallagher[8] developed a thin-walled, open-section beam finite element by expressing the axial displacements in linear polynomial form, and the transverse deflections as well as twist in fifth order Hermite polynomials. This resulted in an element with 10 degrees of freedom (DOF) per node, which is suited for isotropic thin-walled open-section beams. Gupta et al.[9] derived a two-noded, 8 DOF per node, beam finite element for laminated anisotropic thin-walled beams with open section. The displacements of the element reference axes were expressed in terms of one-dimensional first-order Hermite interpolation polynomials, and undeformable cross-section assumptions were invoked in the formulation of the stiffness matrix.

All of the thin-walled elements just mentioned are based on two assumptions: the contour does not deform in its own plane, and the shear strain of the middle surface vanishes for open-section beams. These assumptions were introduced by Vlasov for isotropic thin-walled beams. They may no longer be applicable to laminated composite thin-walleld beams. The thin-walled element developed here is based on a generalized second assumption, using modified stiffnesses to amend the first assumption. Moreover, the thin-walled element presented here is suitable for either open-section or closed-section beams of any shape, and there are no restrictions on the stacking sequence and boundary conditions. In the evaluative examples, shell finite elements are used to model thin-walled structures, and the solutions are compared with those obtained by using thin-walled beam elements.

Received Jan. 18, 1990; revision received May 4, 1990; accepted for publication May 11, 1990.

*Research Associate, School of Aeronautics and Astronautics.
†Professor, School of Aeronautics and Astronautics. Associate Fellow AIAA.

Geometrical Relationships

Let (x,y,z) be a fixed Cartesian coordinate system, with the z axis parallel to the axis of the beam. The plane normal to the longitudinal axis z cuts the middle surface of the beam cross section with a curved line called the contour. A local contour coordinate system (n,s,z), as shown in Fig. 1, is placed on the middle surface where n and s are normal and tangential directions to the contour, respectively. In Fig. 2, point O is the initial point along the contour line coordinate s, and point P is called the pole. The axis through the pole is parallel to the z axis and is called the pole axis. In the present formulation, the location of the pole is arbitrary. Let an auxiliary Cartesian coordinate system $(\bar{n},\bar{s})$ with axes parallel to the directions of n and s at A be placed at P. Thus, the coordinates of point A in the $(\bar{n},\bar{s})$ coordinate system will be r and q. The coordinate system (n,s,z) can be made parallel to the system (x,y,z) by rotating through an angle $(\theta-\pi/2)$.

To derive the finite element for a laminated composite thin-walled beam, the following assumptions are made.

Assumption 1. The thin wall contour does not deform in its own plane. According to this assumption, the displacement components $\bar{u}$ (along the n direction) and $\bar{v}$ (along the s direction) at point A in the contour coordinate system can be expressed in terms of displacements U, V of the pole P in the x, y directions, respectively, and the rotation angle Φ about the pole axis, i.e.,

$$\bar{u}(s,z) = U(z)\sin\theta(s) - V(z)\cos\theta(s) - \Phi(z)\,q(s) \tag{1a}$$

$$\bar{v}(s,z) = U(z)\cos\theta(s) + V(z)\sin\theta(s) + \Phi(z)\,r(s) \tag{1b}$$

Assumption 1 is particularly valid if the cross section of the thin-walled beam is stiffened by closely spaced ribs.

Assumption 2. The axial displacement $\bar{w}$ on the contour can be expressed in the following form:

$$\bar{w}(s,z) = W(z) + \xi(z)x(s) + \eta(z)y(s) + \Psi(z)\omega(s) \tag{2}$$

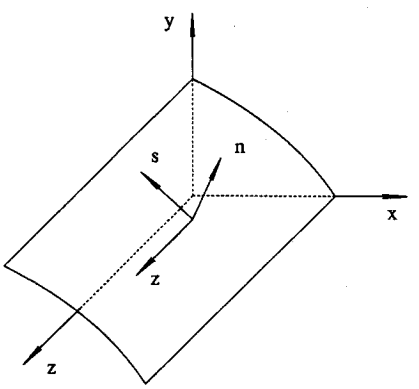

Fig. 1 Coordinate systems for thin-walled beams.

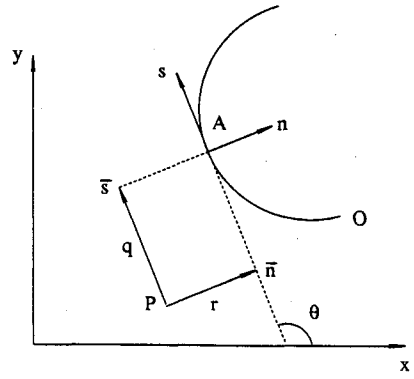

Fig. 2 Definition of coordinates.

where W represents the average axial displacement of the beam in the z direction; x and y are the coordinates of the contour in the (x,y,z) coordinate system; and ω is the so-called sectorial coordinate or warping function, which can be determined by

$$\omega(s) = \int r(s)\, ds \tag{3}$$

for open sections, or

$$\omega(s) = \int \left[r(s) - \frac{F(s)}{h(s)} \right] ds \tag{4}$$

for closed sections. In Eq. (4), F is the St. Venant shear flow,[3] and h the wall thickness. In the classical theory of thin-walled beams, $\xi = -U'$, $\eta = -V'$, and $\Psi = -\Phi'$, in which a prime indicates differentiation with respect to z. The expression given by Eq. (2) allows transverse shear deformations.

Assumption 3. The Kirchhoff-Love assumption in the classical shell theory remains valid for laminated composite thin-walled beams. The displacements of a point off the middle surface of the wall follow from assumption 3, that is,

$$u = \bar{u}, \qquad v = \bar{v} - \left(\frac{\partial \bar{u}}{\partial s} - \frac{\bar{v}}{a} \right) \zeta, \qquad w = \bar{w} - \frac{\partial \bar{u}}{\partial z}\, \zeta \tag{5}$$

where ζ is the thickness coordinate (in the n direction) and $a(s)$ is the radius of curvature of the contour, defined to be positive when the center of curvature lies on the negative n axis.

The strains across the wall thickness are given by

$$\epsilon_s = \frac{\epsilon_{s0} - \zeta \chi_s}{1 + (\zeta/a)}, \qquad \epsilon_z = \epsilon_{z0} - \zeta \chi_z, \qquad \gamma_{sz} = \frac{\mu_{zs} - \zeta \kappa_{zs}}{1 + (\zeta/a)} + \mu_{sz} - \zeta \kappa_{sz} \tag{6}$$

where

$$\epsilon_{z0} = \frac{\partial \bar{w}}{\partial z}, \qquad \epsilon_{s0} = \frac{\partial \bar{v}}{\partial s} + \frac{\bar{u}}{a} \tag{7a}$$

$$\mu_{sz} = \frac{\partial \bar{v}}{\partial z}, \qquad \mu_{zs} = \frac{\partial \bar{w}}{\partial s} \tag{7b}$$

$$\chi_z = \frac{\partial^2 \bar{u}}{\partial z^2}, \qquad \chi_s = \frac{\partial}{\partial s}\left(\frac{\partial \bar{u}}{\partial s} - \frac{\bar{v}}{a} \right) \tag{7c}$$

$$\kappa_{sz} = \frac{\partial}{\partial z}\left(\frac{\partial \bar{u}}{\partial s} - \frac{\bar{v}}{a} \right), \qquad \kappa_{zs} = \frac{\partial^2 \bar{u}}{\partial z\, \partial s} \tag{7d}$$

Finite Element Formulation

The wall thickness of the laminated beam is built up of an arbitrary number of bonded orthotropic layers having different thicknesses and fiber orientations. The stresses and the strains with respect to the structural principal axes (n,s,z) in each layer are related by

$$\begin{Bmatrix} \sigma_z \\ \sigma_s \\ \tau_{zs} \end{Bmatrix}_k = \begin{bmatrix} \bar{Q}_{11} & \bar{Q}_{12} & \bar{Q}_{16} \\ \bar{Q}_{12} & \bar{Q}_{22} & \bar{Q}_{26} \\ \bar{Q}_{16} & \bar{Q}_{26} & \bar{Q}_{66} \end{bmatrix} \begin{Bmatrix} \epsilon_z \\ \epsilon_s \\ \gamma_{zs} \end{Bmatrix}_k \tag{8}$$

where $\bar{Q}_{ij}$ are the reduced stiffnesses of the unidirectional fiber composite relative to the (n,s,z) coordinates.[10] The resultant forces and moments can be expressed as

$$\begin{Bmatrix} N_z \\ N_s \\ N_{zs} \\ N_{sz} \\ M_z \\ M_s \\ M_{zs} \\ M_{sz} \end{Bmatrix} = [\bar{S}] \begin{Bmatrix} \epsilon_{z0} \\ \epsilon_{s0} \\ \mu_{sz} \\ \mu_{zs} \\ -\chi_z \\ -\chi_s \\ -\kappa_{sz} \\ -\kappa_{zs} \end{Bmatrix} \tag{9}$$

where

$$N_z = \int \sigma_z \left(1 + \frac{\zeta}{a} \right) d\zeta, \qquad N_s = \int \sigma_s\, d\zeta \tag{10a}$$

$$N_{zs} = \int \tau_{zs} \left(1 + \frac{\zeta}{a} \right) d\zeta, \qquad N_{sz} = \int \tau_{sz}\, d\zeta \tag{10b}$$

$$M_z = \int \sigma_z \left(1 + \frac{\zeta}{a} \right) \zeta\, d\zeta, \qquad M_s = \int \sigma_s \zeta\, d\zeta \tag{10c}$$

$$M_{zs} = \int \tau_{zs} \left(1 + \frac{\zeta}{a} \right) \zeta\, d\zeta, \qquad M_{sz} = \int \tau_{sz} \zeta\, d\zeta \tag{10d}$$

are the resultant forces and moments over the wall thickness, and

$$[\bar{S}] = \begin{bmatrix} \bar{A} & \bar{B} \\ \bar{B} & \bar{D} \end{bmatrix} \tag{11}$$

in which

$$[\bar{A}] = \begin{bmatrix} Q_{11}^{(0)} + \dfrac{Q_{11}^{(1)}}{a} & Q_{12}^{(0)} & Q_{16}^{(0)} + \dfrac{Q_{16}^{(1)}}{a} & Q_{16}^{(0)} \\ Q_{12}^{(0)} & Q_{22}^{(0)} - \dfrac{Q_{22}^{(1)}}{a} & Q_{26}^{(0)} & Q_{26}^{(0)} - \dfrac{Q_{26}^{(1)}}{a} \\ Q_{16}^{(0)} + \dfrac{Q_{16}^{(1)}}{a} & Q_{26}^{(0)} & Q_{66}^{(0)} + \dfrac{Q_{66}^{(1)}}{a} & Q_{66}^{(0)} \\ Q_{16}^{(0)} & Q_{26}^{(0)} - \dfrac{Q_{26}^{(1)}}{a} & Q_{66}^{(0)} & Q_{66}^{(0)} - \dfrac{Q_{66}^{(1)}}{a} \end{bmatrix} \tag{12a}$$

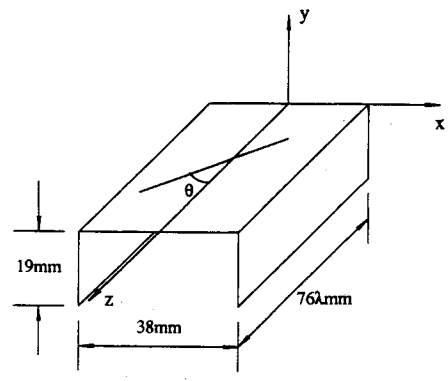

Fig. 3 Geometry of thin-walled channel.

$$[\bar{B}] = \begin{bmatrix} Q_{11}^{(1)} + \frac{Q_{11}^{(2)}}{a} & Q_{12}^{(1)} & Q_{16}^{(1)} + \frac{Q_{16}^{(2)}}{a} & Q_{16}^{(1)} \\ Q_{12}^{(1)} & Q_{22}^{(1)} - \frac{Q_{22}^{(2)}}{a} & Q_{26}^{(1)} & Q_{26}^{(1)} - \frac{Q_{26}^{(2)}}{a} \\ Q_{16}^{(1)} + \frac{Q_{16}^{(2)}}{a} & Q_{26}^{(1)} & Q_{66}^{(1)} + \frac{Q_{66}^{(2)}}{a} & Q_{66}^{(1)} \\ Q_{16}^{(1)} & Q_{26}^{(1)} - \frac{Q_{26}^{(2)}}{a} & Q_{66}^{(1)} & Q_{66}^{(1)} - \frac{Q_{66}^{(2)}}{a} \end{bmatrix} \tag{12b}$$

$$[\bar{D}] = \begin{bmatrix} Q_{11}^{(2)} + \frac{Q_{11}^{(3)}}{a} & Q_{12}^{(2)} & Q_{16}^{(2)} + \frac{Q_{16}^{(3)}}{a} & Q_{16}^{(2)} \\ Q_{12}^{(2)} & Q_{22}^{(2)} - \frac{Q_{22}^{(3)}}{a} & Q_{26}^{(2)} & Q_{26}^{(2)} - \frac{Q_{26}^{(3)}}{a} \\ Q_{16}^{(2)} + \frac{Q_{16}^{(3)}}{a} & Q_{26}^{(2)} & Q_{66}^{(2)} + \frac{Q_{66}^{(3)}}{a} & Q_{66}^{(2)} \\ Q_{16}^{(2)} & Q_{26}^{(2)} - \frac{Q_{26}^{(3)}}{a} & Q_{66}^{(2)} & Q_{66}^{(2)} - \frac{Q_{66}^{(3)}}{a} \end{bmatrix} \tag{12c}$$

and

$$Q_{ij}^{(0)} = \int \bar{Q}_{ij}\, d\zeta \tag{13a}$$

$$Q_{ij}^{(1)} = \int \bar{Q}_{ij}\, \zeta\, d\zeta \tag{13b}$$

$$Q_{ij}^{(2)} = \int \bar{Q}_{ij}\, \zeta^2\, d\zeta \tag{13c}$$

$$Q_{ij}^{(3)} = \int \bar{Q}_{ij}\, \zeta^3\, d\zeta \tag{13d}$$

According to Assumption 1, it can be shown that

$$\epsilon_{s0} = 0, \qquad \chi_s = 0 \tag{14}$$

Deleting the second and sixth rows and columns in Eq. (9), we have

$$\{N\} = [S]^*\{\epsilon\} \tag{15}$$

where $[S]^*$ is reduced from $[S]$, and

$$\{N\} = \{N_z\ N_{zs}\ N_{sz}\ M_z\ M_{zs}\ M_{sz}\}^T \tag{16}$$

$$\{\epsilon\} = \{\epsilon_{z0}\ \mu_{sz}\ \mu_{zs}\ -\chi_z\ -\kappa_{sz}\ -\kappa_{zs}\}^T \tag{17}$$

The conditions of Eq. (14) are not always true unless the cross sections are stiffened by very closely spaced ribs. If there are no ribs, it may be more reasonable to assume

$$N_s = M_s = 0 \tag{18}$$

By using Eq. (18), the constitutive equation (9) can be reduced by solving for ϵ_{s0} and χ_s with $N_s = M_s = 0$, and then eliminating ϵ_{s0} and χ_s from Eq. (9). We have

$$\{N\} = [S]^{**}\{\epsilon\} \tag{19}$$

The actual stiffness should lie between the preceeding two extreme cases. In view of the foregoing, we take

$$\{N\} = [S]\{\epsilon\} \tag{20}$$

with

$$[S] = (1-\delta)[S]^* + \delta[S]^{**} \tag{21}$$

where δ takes a value between 0 and 1. For slender thin-walled beams without ribs, $\delta = 1$ should yield more accurate results.

The strain energy of the element is

$$U = \frac{1}{2}\int_0^L \int_0^S \int_{-h/2}^{h/2} (\sigma_z \epsilon_z + \sigma_s \epsilon_s + \tau_{zs}\gamma_{zs})\left(1 + \frac{\zeta}{a}\right) d\zeta\, ds\, dz$$

$$= \frac{1}{2}\int_0^L \int_0^S \{N\}^T \{\epsilon\}\, ds\, dz \tag{22}$$

where L is the length of the element, S the length of the contour, and h the thickness of the wall. By substituting Eqs. (1) and (2) into Eqs. (7), $\{\epsilon\}$ can be written as

$$\{\epsilon\} = [B]\{\Delta^*\} \tag{23}$$

where

$$[B] = \begin{bmatrix} 1 & x & y & \omega & 0 & 0 & 0 & 0 & 0 & 0 & 0 & 0 \\ 0 & 0 & 0 & 0 & c\theta & s\theta & r & 0 & 0 & 0 & 0 & 0 \\ 0 & 0 & 0 & 0 & 0 & 0 & 0 & \dot{x} & \dot{y} & \dot{\omega} & 0 & 0 \\ 0 & 0 & 0 & 0 & 0 & 0 & 0 & 0 & 0 & 0 & -s\theta & c\theta \\ 0 & 0 & 0 & 0 & 0 & 0 & 1 & 0 & 0 & 0 & 0 & 0 \\ 0 & 0 & 0 & 0 & -\frac{c\theta}{a} & -\frac{s\theta}{a} & 1-\frac{r}{a} & 0 & 0 & 0 & 0 & 0 \end{bmatrix} \begin{matrix} 0 \\ 0 \\ 0 \\ q \\ 0 \\ 0 \end{matrix} \tag{24}$$

in which $s\theta$ and $c\theta$ denote $\sin\theta$ and $\cos\theta$, respectively, a dot represents differentiation with respect to s, and

$$\{\Delta^*\} = \{W'\ \xi'\ \eta'\ \Psi'\ U'\ V'\ \Phi'\ \xi\ \eta\ \Psi\ U''\ V''\ \Phi''\}^T \tag{25}$$

in which a prime indicates differentiation with respect to z.

The generalized displacements of the beam are expressed in terms of one-dimensional Hermite interpolation polynomials as

$$W = H_1 W_1 + H_2 W_2 \tag{26a}$$

$$\xi = H_1 \xi_1 + H_2 \xi_2 \tag{26b}$$

$$\eta = H_1 \eta_1 + H_2 \eta_2 \tag{26c}$$

$$\Psi = H_1 \Psi_1 + H_2 \Psi_2 \tag{26d}$$

$$U = H_{01} U_1 + H_{02} U_2 + H_{11} U_1' + H_{12} U_2' \tag{26e}$$

$$V = H_{01} V_1 + H_{02} V_2 + H_{11} V_1' + H_{12} V_2' \tag{26f}$$

$$\Phi = H_{01} \Phi_1 + H_{02} \Phi_2 + H_{11} \Phi_1' + H_{12} \Phi_2' \tag{26g}$$

where

$$H_1 = 1 - z/L \tag{27a}$$

$$H_2 = z/L \tag{27b}$$

$$H_{01} = (2z^3 - 3Lz^2 + L^3)/L^3 \tag{27c}$$

$$H_{02} = (-2z^3 + 3Lz^2)/L^3 \tag{27d}$$

$$H_{11} = (z^3 - 2Lz^2 + L^2 z)/L^2 \tag{27e}$$

$$H_{12} = (z^3 - Lz^2)/L^2 \tag{27f}$$

Thus, $\{\Delta^*\}$ can be expressed in terms of nodal displacements $\{\Delta\}$ as

$$\{\Delta^*\} = [H]\{\Delta\} \tag{28}$$

where

$$\{\Delta\} = \{W_1\ \xi_1\ \eta_1\ \Psi_1\ U_1\ V_1\ \Phi_1\ U_1'\ V_1'\ \Phi_1'$$
$$W_2\ \xi_2\ \eta_2\ \Psi_2\ U_2\ V_2\ \Phi_2\ U_2'\ V_2'\ \Phi_2'\}^T \quad (29)$$

Substituting Eqs. (20) and (23) in the strain energy expression (22), we obtain

$$U = \tfrac{1}{2}\{\Delta\}^T\int_0^L[H]^T\int_0^S[B]^T[S][B]\ ds\ [H]\ dz\{\Delta\}$$
$$= \tfrac{1}{2}\{\Delta\}^T\ [K]\ \{\Delta\} \quad (30)$$

where

$$[K] = \int_0^L[H]^T[D][H]\ dz \quad (31)$$

is the element stiffness matrix, and

$$[D] = \int_0^S[B]^T[S][B]\ ds \quad (32)$$

depends on the shape of the cross section and the laminate construction.

To derive the mass matrix of a thin-walled beam element, we neglect the inertia associated with the shearing of the wall. Thus, the kinetic energy of the element can be written as

$$T = \frac{1}{2}\int_0^L\int_0^S\left\{\frac{\partial\bar{u}}{\partial t}\right\}^T\rho h\left\{\frac{\partial\bar{u}}{\partial t}\right\}ds\ dz \quad (33)$$

where o is the density, t the time variable, and

$$\{\bar{u}\} = \begin{Bmatrix}\bar{u}\\ \bar{v}\\ \bar{w}\end{Bmatrix} = \begin{bmatrix}0&0&0&0&\sin\theta&-\cos\theta&-q\\ 0&0&0&0&\cos\theta&\sin\theta&r\\ 1&x&y&\omega&0&0&0\end{bmatrix}\begin{Bmatrix}W\\ \xi\\ \eta\\ \Psi\\ U\\ V\\ \Phi\end{Bmatrix} = [C]\{W\} \quad (34)$$

By Eqs. (26), $\{W\}$ can be expressed in terms of nodal displacement as

$$\{W\} = [H^*]\{\Delta\} \quad (35)$$

Thus, the kinetic energy can be written as

$$T = \frac{1}{2}\left\{\frac{d\Delta}{dt}\right\}^T[M]\left\{\frac{d\Delta}{dt}\right\} \quad (36)$$

where $[M]$ is the mass matrix, given by

$$[M] = \int_0^L[H^*]^T[m][H^*]\ dz \quad (37)$$

in which

$$[m] = \int_0^S[C]^T\rho h[C]\ ds \quad (38)$$

Table 1 Frequencies (Hz) of 76 × 76 mm eight-ply square plates

Laminate	Mode	Experiment[11]	Shell element[11]	MARC	Thin-walled element $\delta = 0$	$\delta = 1$	$\delta = 0.3$
$[0_2/\pm 30]_s$	1B	234.2	261.9	261.7	262.0	259.5	261.3
	1T	362.0	363.5	364.4	370.5	367.1	369.5
	1C	728.3	761.8	762.2			
	2B	1449.0	1662.0	1641.0	1644.0	1628.0	1639.0
	2C	1503.0	1709.0	1730.0			
$[0/\pm 45/90]_s$	1B	196.4	224.3	224.3	225.8	215.7	222.9
	1T	418.0	421.8	424.5	437.9	420.8	432.9
	1C	960.0	1012.0	1017.0			
	2B	1215.0	1426.0	1414.0	1418.0	1353.0	1399.0
	2T	1550.0	1722.0	1722.0	1771.0	1695.0	1748.0
$[\pm 45/\mp 45]_s$	1B	131.2	138.9	140.2	150.7	94.8	136.4
	1T	472.0	499.5	505.6	511.7	472.1	501.3
	2B	790.5	805.0	810.6	948.1	594.4	857.8
	1C	1168.0	1326.0	1331.0			
	2T	1486.0	1648.0	1666.0	1737.0	1513.0	1677.0

Table 2 Frequencies (Hz) of 152 × 76 mm eight-ply rectangular plates

Laminate	Mode	Experiment[11]	Shell element[11]	MARC	Thin-walled element $\delta = 0$	$\delta = 1$	$\delta = 0.5$
$[0_2/\pm 30]_s$	1B	58.3	65.37	65.28	65.46	64.84	65.17
	1T	148.0	137.5	137.7	139.2	138.1	138.7
	2B	362.7	408.3	408.0	410.9	406.8	408.9
	2T	508.0	525.6	526.3	540.5	535.5	538.0
	1C	546.0	588.3	582.9			
$[0/\pm 45/90]_s$	1B	48.6	55.58	55.55	56.36	53.91	55.12
	1T	169.0	175.4	176.1	180.9	174.2	177.7
	2B	303.0	345.3	345.4	354.4	338.1	346.4
	2T	554.0	591.8	595.8	621.1	597.7	609.8
	1C	739.0	820.1	814.0			
$[\pm 45/\mp 45]_s$	1B	31.3	31.90	32.32	37.61	23.69	31.50
	2B	185.8	191.3	193.7	226.0	148.4	196.6
	1T	214.0	228.2	230.5	242.7	222.5	228.8
	3B	533.0	565.3	571.5	651.1	415.8	551.1
	2T	653.0	708.3	717.3	742.7	682.3	710.8

Examples and Discussion

To evaluate the performance of the composite thin-walled beam element, we compared our results with those given by Crawley.[11] Crawley considered graphite/epoxy laminated plates of aspect ratios λ (length of the beam divided by length of contour) 1 and 2, measuring 76×76 mm ($\lambda = 1$) and 152×76 mm ($\lambda = 2$), respectively, and a similar set of 152×76 mm ($\lambda = 2$) cylindrical panels with a radius of curvature of 127 mm. However, Crawley did not provide results with an aspect ratio $\lambda > 2$. To investigate the validity of the thin-walled beam element for slender beams, the MARC general purpose finite element program, developed by MARC Analysis Research Corporation, was used to calculate the natural frequencies of additional plates and channels. To test laminates that are stiff in bending, stiff in torsion, or quasi-isotropic, the following eight-ply laminates were chosen: bending stiff $[0_2/\pm 30]_s$, quasi-isotropic $[0/\pm 45/90]_s$, and torsion stiff $[\pm 45/\mp 45]_s$.

The shell element used by Crawley was a moderately thick, general quadrilateral, shallow shell element with eight nodes and 5 DOF per node. The 3×3 grids were used for the plate with an aspect ratio of 1, and 6×3 for the plate with an aspect ratio of 2. Whereas only eight thin-walled elements were used for both plates, the total degrees of freedom were 160, which were less than 720 DOF for the 6×3 shell element model. In using the MARC program, a rectangular doubly curved shell element was chosen, which has four nodes and 12 DOF per node. The 2×10 grids were used for the plates and 3×10 for the channels. In contrast with the MARC program, 10 thin-walled elements were used for the plates with $\lambda > 2$ and for the channels. In these cases, the beams were divided uniformly into 10 elements along the axis of the beam.

Table 3 Frequencies (Hz) of 304×76 mm eight-ply rectangular plates

			Thin-walled element		
Laminate	Mode	MARC	$\delta = 0$	$\delta = 1$	$\delta = 0.65$
$[0_2/\pm 30]_s$	1B	16.27	16.34	16.19	16.25
	1T	58.16	58.60	58.13	58.30
	2B	102.0	102.7	101.7	102.0
	2T	194.8	196.9	195.3	195.9
	3B	286.2	288.2	285.2	286.3
$[0/\pm 45/90]_s$	1B	13.74	14.06	13.47	13.69
	1T	78.86	80.54	78.22	79.09
	2B	86.03	89.35	84.71	86.35
	3B	239.1	241.1	235.0	237.4
	2T	251.8	264.5	249.6	254.7
$[\pm 45/\mp 45]_s$	1B	7.334	9.390	5.921	7.340
	2B	45.40	58.80	37.11	45.99
	1T	110.0	111.2	103.9	109.3
	3B	133.8	164.7	108.2	128.8
	4B	275.5	322.8	203.8	252.6

Table 4 Frequencies (Hz) of 608×76 mm eight-ply rectangular plates

			Thin-walled element		
Laminate	Mode	MARC	$\delta = 0$	$\delta = 1$	$\delta = 0.82$
$[0_2/\pm 30]_s$	1B	4.056	4.081	4.045	4.051
	2B	25.16	25.26	25.10	25.13
	1T	26.83	27.13	26.82	26.88
	3B	70.86	71.19	70.67	70.77
	2T	83.50	84.39	83.52	83.67
$[0/\pm 45/90]_s$	1B	3.408	3.512	3.367	3.395
	2B	21.33	21.99	21.10	21.27
	1T	37.49	38.87	37.35	37.63
	3B	59.81	61.57	59.09	59.57
	2T	114.3	118.5	113.8	114.7
$[\pm 45/\mp 45]_s$	1B	1.685	2.346	1.480	1.672
	2B	10.60	14.70	9.276	10.48
	3B	30.63	41.17	25.98	29.35
	1T	53.90	54.45	50.94	53.70
	4B	62.60	80.74	53.54	57.57

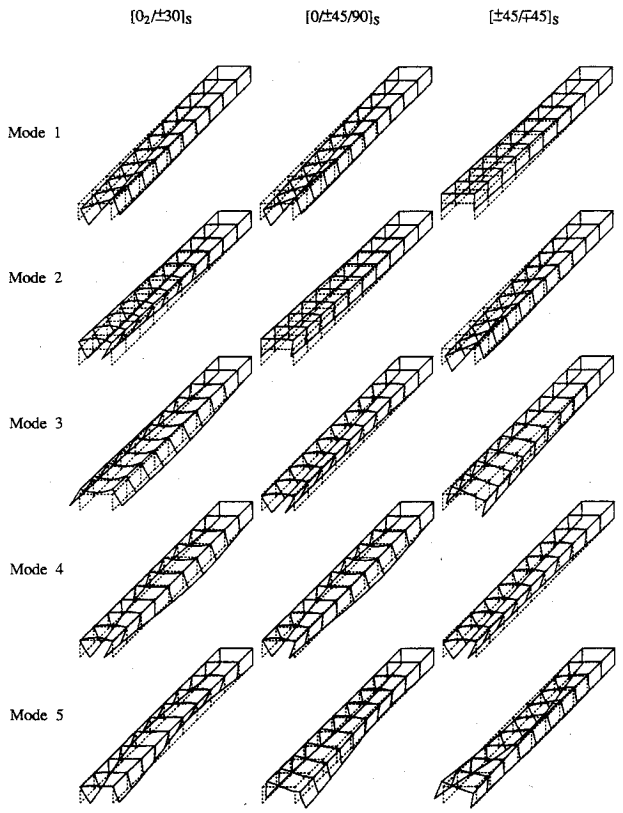

Fig. 4 Mode shapes for channels with $\lambda = 3$.

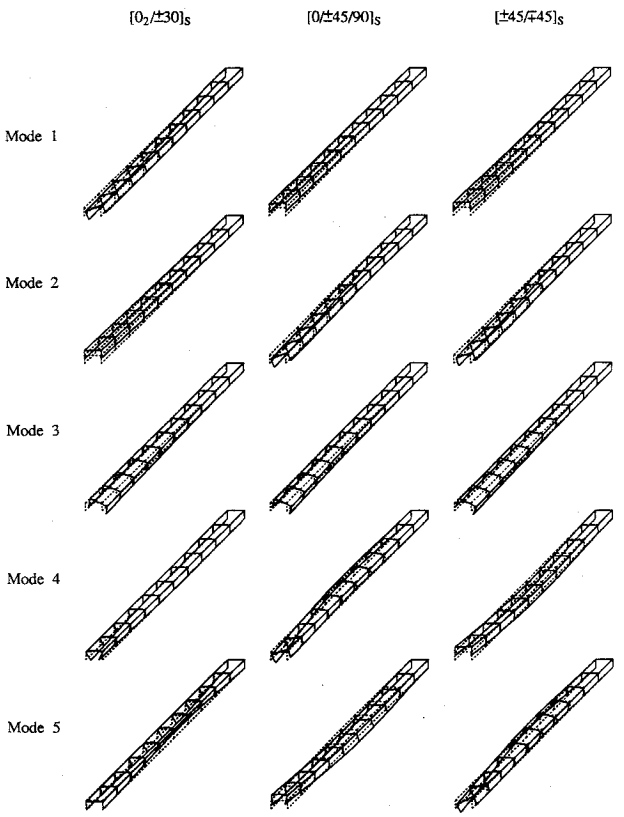

Fig. 5 Mode shapes for channels with $\lambda = 6$.

Table 5 Frequencies (Hz) of 152 × 76 mm eight-ply cylindrical panels

Laminate	Mode	Experiment[11]	Shell element[11]	Thin-walled element $\delta = 0$	Thin-walled element $\delta = 1$
$[0_2/\pm 30]_s$	1T	161.0	165.7	172.6	168.3
	1B	254.1	289.6	325.3	307.5
	1C	555.6	597.1		
	2T	670.0	718.5	758.8	737.2
$[0/\pm 45/90]_s$	1T	177.0	192.4	202.2	194.1
	1B	201.8	236.1	247.7	235.8
	2T	645.0	705.8	755.3	724.1
	1C	754.0	808.2		
$[\pm 45/\mp 45]_s$	1B	145.3	147.0	213.5	134.5
	1T	222.0	238.0	252.0	232.8
	2T	712.0	768.1	845.3	743.4
	2B	774.2	812.1	1261.0	822.6

Table 6 Frequencies (Hz) of 76 × 76 mm eight-ply cantilever channels

Laminate	Mode $\lambda = 3$	Mode $\lambda = 6$	MARC $\lambda = 3$	MARC $\lambda = 6$	Thin-walled element, $\delta = 1$ $\lambda = 3$	Thin-walled element, $\delta = 1$ $\lambda = 6$
$[0_2/\pm 30]_s$	1TB[a]	1TB	386.5	108.0	397.7	107.9
	1BC[b]	1B	452.4	127.8	502.9	127.7
	2BC	2TB	614.7	386.8		391.2
	1C	1C	701.1	529.9		
	2C	2C	942.6	532.0		
$[0/\pm 45/90]_s$	1TB	1B	316.3	95.36	318.5	95.11
	1B	1TB	372.1	96.88	377.5	97.26
	1C	2TB	811.5	298.6		299.4
	2C	3TB	965.6	476.9		486.1
	2TB	2B	1048.0	561.6	1122.0	588.7
$[\pm 45/\mp 45]_s$	1B	1B	224.3	55.96	214.8	53.83
	1TB	1TB	250.4	91.64	247.6	89.93
	2TB	2TB	692.2	190.7	678.5	185.3
	1C	2B	1017.0	347.6		336.7
	3TB	3TB	1136.0	367.4	1145.0	362.4

[a]TB = Coupled torsion-bending mode.
[b]BC = Coupled bending-chordwise mode.

Table 7 Frequencies (Hz) for the 228 × 76 mm $[0_2/\pm 30]_s$ cantilever channels stiffened by massless diaphragms

Thin-walled element $\delta = 0$	Thin-walled element $\delta = 1$	MARC $(E/E_1) = 1$
422.5	397.7	401.1
535.2	502.9	505.7
1484.0	1412.0	1422.0
2402.0	2275.0	2249.0
2982.0	2835.0	2725.0

In all of the examples, the thin-walled beam was assumed to be clamped at one end and free at another end.

The material properties of the composite used in the finite element calculation are: $E_1 = 128.0$ GPa, $E_2 = 11.0$ GPa, $\nu_{12} = 0.25$, $G_{12} = 4.48$ GPa, ρ (density) $= 1.5 \times 10^3$ Kg/m^3, and ply thickness = 0.13 mm.

Plates

Tables 1–4 present the results for the plates with aspect ratios $\lambda = 1$, 2, 4, and 8, respectively. It is seen that there are no corresponding frequencies of chordwise modes, which are indicated by 1C, 2C, etc., for the thin-walled element. This is because the thin-walled element does not include the distortion of the cross section according to Assumption 1. However, as the aspect ratio increases, chordwise modes tend to appear as higher modes, when compared with bending and torsional modes which are indicated by 1B, 2B and 1T, 2T, respectively.

From the results presented in Tables 1–4, it is evident that the thin-walled finite element solutions with $\delta = 0$ and 1 give the upper and lower bounds of the frequency, respectively. It is interesting to note that for the $[0_2/\pm 30]_s$ and $[0/\pm 45/90]_s$ laminates, the difference between the bounds is very small, and either solution is fairly accurate as compared with the shell finite element solutions.

The results for the $[\pm 45/\mp 45]_s$ laminated plate indicate that the bound between the two solutions with $\delta = 0$ and 1 is large and that the solution is sensitive to the choice of δ. In general, for plates with larger aspect ratios, the value of δ approaches unity.

Cylindrical Panels

Table 5 lists the frequencies for the cylindrical panels with a radius of curvature of 127 mm. It is evident that $\delta = 1$ yields fairly good results for all laminates considered.

Channels

The geometry of the channel is shown in Fig. 3. Ply angle θ is the angle between the fiber direction and the z direction. Figures 4 and 5 show the sketches of the first five natural modes for each channel considered. These mode shapes were obtained using the MARC program. It is noted that, for $\lambda = 3$, the chordwise mode may appear. As the aspect ratio increases, the chordwise modes are pushed into higher vibration modes (see Fig. 5). Among the three stacking sequences, $[0_2/\pm 30]_s$ is most likely to produce chordwise modes. The $[\pm 45/\mp 45]_s$ laminate best obeys the basic assumptions for the thin-walled beam.

The natural frequencies for the channels are listed in Table 6. The value $\delta = 1$ yields fairly good solutions with the thin-walled beam element. In fact, based on the results of Tables 5 and 6, $\delta = 1$ seems to be suitable for curved panels and channels. Note that, for the $[0_2/\pm 30]_s$ channel with $\lambda = 3$, the second and third modes in the MARC solution are coupled bending-chordwise modes, whereas the second mode produced by the thin-walled beam element is a bending mode; see Table 6.

Diaphragm-Stiffened Channels

The thin-walled element usually gives better results when the aspect ratio is large. This is because the thin-walled element does not take into account the distortion of the cross section, which dominates the lower modes when the aspect ratio is not large. It is evident that the thin-walled element should yield good approximate solutions if the cross section of the thin wall is stiffened by ribs or diaphragms, which suppress the distortion of the cross section. In view of the foregoing, we consider the $[0_2/\pm 30]_2$ channel with $\lambda = 3$ stiffened by 10 massless diaphragms, which are equally spaced along the axis of the beams. The diaphragms are 18 × 36 mm isotropic plates, each of which is taken as one element. The Young's modulus of the diaphragms is denoted by E, the Poisson ratio is 0.25, and the thickness is 1.04 mm. The results of the thin-walled element are compared with those obtained from the MARC program in Table 7. It is evident that the thin-walled element solutions with $\delta = 1$ agree well with the MARC solutions.

Conclusion

A two-noded, 10 DOF, thin-walled finite element for laminated composite beam-like structures was developed based on modified assumptions of classical isotropic thin-walled beam theory. The performance of this element was evaluated by comparing the results with those given by the shell element. This comparison indicated that for thin-walled beams with large aspect ratios, the chordwise modes are not present among the lower modes, and the thin-wall beam theory (with

$\delta = 1$) yielded excellent natural frequencies. The use of diaphragms to prevent distortion of the cross section of a channel would also make the thin-walled beam theory suitable for analysis of thin-walled structures with smaller aspect ratios.

References

[1]Vlasov, V. Z., *Thin-Walled Elastic Beams,* National Science Foundation, Washington, DC, U.S. Dept. of Commerce, Washington, DC, and Israeli Programme for Science Translations, Jerusalem, 1961 (translated from Russian).

[2]Timoshenko, S. P., "Theory of Bending, Torsion and Buckling of Thin-Walled Members of Open Cross-Section," *Journal of the Franklin Institute*, Vol. 239, No. 3, 1945, pp. 201–219.

[3]Gjelsvik, A., *The Theory of Thin-Walled Bars,* Wiley, New York, 1981.

[4]Bauld, N. R., Jr., and Tzeng, L. S., "A Vlasov Theory for Fiber-Reinforced Beams with Thin-Walled Open Cross Sections," *International Journal of Solid & Structures*, Vol. 20, No. 3, 1984, pp. 277–297.

[5]Krahula, J. L., "Analysis of Bent and Twisted Bars Using Finite Element Method," *AIAA Journal*, Vol. 5, No. 6, 1967, pp. 1194–1197.

[6]Krajcinovic, D., "A Consistent Discrete Element Technique for Thin-Walled Assemblages," *International Journal of Solid & Structures*, Vol. 5, No. 7, 1969, pp. 629–632.

[7]Yoo, C. H., "Matrix Formulation of Curved Girders," *Journal of Engineering Mechanics Division, Proceedings of the ASCE, EM6,* Vol. 105, 1979, pp. 971–988.

[8]Barsoum, R. S., and Gallagher, R. H., "Finite Element Analysis of Torsional Flexural Stability Problems," *International Journal for Numerical Methods in Engineering*, Vol. 2, No. 3, 1970, pp. 335–352.

[9]Gupta, R. K., Venkatesh, A., and Rao, K. P., "Finite Element Analysis of Laminated Anisotropic Thin-Walled Open-Section Beams," *Composite Structures*, Vol. 3, 1985, pp. 19–31.

[10]Jones, R. M., *Mechanics of Composite Materials,* Scripta, Washington, DC, 1975.

[11]Crawley, E. F., "The Natural Modes of Graphite/Epoxy Cantilever Plates and Shell" *Journal of Composite Materials*, Vol. 13, No. 3, July 1979, pp. 195–205.